THE JOURNAL OF PHYSICAL CHEMISTRY B

Article

pubs.acs.org/JPCB

Thermodynamics-Hydration Relationships within Loops That Affect G-Quadruplexes under Molecular Crowding Conditions

Takeshi Fujimoto,[†] Shu-ichi Nakano,[†,‡] Naoki Sugimoto,*[,†,‡] and Daisuke Miyoshi*[,†,‡]

[†]Faculty of Frontiers of Innovative Research in Science and Technology (FIRST), and [‡]Frontier Institute for Biomolecular Engineering Research (FIBER), Konan University, 7-1-20, Minatojima-minamimachi, Chuo-ku, Kobe 650-0047, Japan

Supporting Information

ABSTRACT: We systematically investigated the effects of loop length on the conformation, thermodynamic stability, and hydration of DNA G-quadruplexes under dilute and molecular crowding conditions in the presence of Na^+. Structural analysis showed that molecular crowding induced conformational switches of oligonucleotides with the longer guanine stretch and the shorter thymine loop. Thermodynamic parameters further demonstrated that the thermodynamic stability of G-quadruplexes increased by increasing the loop length from two to four, whereas it decreased by increasing the loop length from four to six. Interestingly, we found by osmotic pressure analysis that the number of water molecules released from the G-quadruplex decreased with increasing thermodynamic stability. We assumed that base-stacking interactions within the loops not only stabilized the whole G-quadruplex structure but also created hydration sites by accumulating nucleotide functional groups. The molecular crowding effects on the stability of G-quadruplexes composed of abasic sites, which reduce the stacking interactions at the loops, further demonstrated that G-quadruplexes with fewer stacking interactions within the loops released a larger number of water molecules upon folding. These results showed that the stacking interactions within the loops determined the thermodynamic stability and hydration of the whole G-quadruplex.

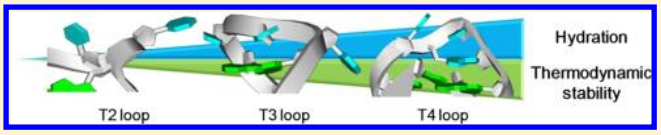

1. INTRODUCTION

Guanine-rich nucleic acid sequences are able to form G-quadruplexes.[1,2] The G-quadruplex is made up of stacked G-quartet subunits, wherein four coplanar guanines are linked together by Hoogsteen hydrogen bonds.[3−5] Stacking interactions among the G-quartets make a stable G-quadruplex structure in the presence of monovalent cations, which fit within the central core of guanine carbonyls.[6,7] Since it has been reported that G-quadruplexes may form at telomeres, oncogene promoters, and other biologically important genomic regions,[8−10] they have received wide attention as attractive therapeutic targets.[11−15] Moreover, G-quadruplexes show unique properties, such as high thermal and biological stabilities, binding affinity for various molecules from metal ions to proteins, and a molecular geometry characterized by a polymorphic nature among various conformations, including antiprallel, parallel, and mixed (Figure 1a). These properties are useful for the design and development of novel functional nanomaterials and nanodevices.[16−24] Therefore, it is important to understand the rules that govern the conformation and thermodynamic stability of G-quadruplexes.

For formation of an intramolecular G-quadruplex, four tracks of two or more guanines and three loops (the first, second, and third loops from the 5′ end) of various sizes and sequences connecting the guanine tracks are required (Figure 1b).[25−27] It has been demonstrated that the conformation of an intramolecular G-quadruplex depends on the loop length.[28−32] Bugaut et al. and Guédin et al. independently analyzed G-quadruplex conformations composed of various lengths of loops by use of circular dichroism (CD).[31,32] They found that the conformation of G-quadruplexes with total loop length shorter than five bases was likely to be parallel (Figure 1a). On the other hand, the conformation of G-quadruplexes with total loop length longer than five bases was likely to be mixed or antiparallel (Figure 1a). It was also reported that the conformation of G-quadruplexes with a first or third loop length of one base is parallel.[30] These results demonstrate the critical role of loop length in the structural polymorphism of the G-quadruplex. Furthermore, the loop length affects the thermodynamics of the G-quadruplex. In general, increasing the total loop length leads to destabilization of the G-quadruplex, although there are some exception. Olsen et al. investigated the thermodynamic contributions of loop sequences using a thrombin binding aptamer (5′-GGTTGGTGTGGTTGG-3′; loops are underlined).[33] They designed modified thrombin binding aptamers containing base substitutions in the TGT and TT loops, and found that the melting temperatures (T_ms) of these aptamers varied from 43.2 to 56.5 °C. Thus, the loop sequence as well as length are important determinants of the thermodynamics of G-quadruplexes.

Moreover, biophysical and structural studies, even by NMR and X-ray crystallography, have shown that the polymorphic nature of G-quadruplexes is induced and regulated not only by the nucleotide sequence, but also by cellular environmental factors including cation species, their concentrations, and molecular crowding.[34−36] Molecular conditions in a living cell

Received: August 23, 2012
Revised: November 12, 2012
Published: November 15, 2012

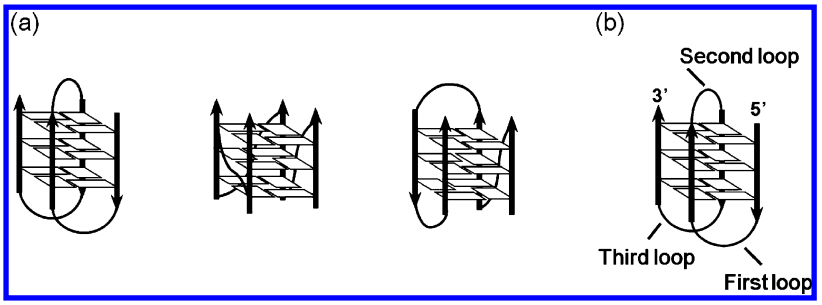

Figure 1. (a) Schematic illustrations of G-quadruplex conformations [antiparallel (left), parallel (middle), and mixed (right)]. (b) Schematic illustration of an intramolecular G-quadruplex with three loops.

and on a material surface are significantly different from those in a homologous aqueous solution. One of the most characteristic features of intracellular conditions is a molecularly crowded environment with biomolecules.[37] Small hydrophilic molecules such as metabolites and osmolytes are also highly crowded in a living cell, resulting in the properties of intracellular water being significantly different from those of a dilute solution.[38] Importantly, molecular crowding causes a drastic change in the conformation and thermodynamics of G-quadruplexes.[39] Moreover, it has been reported that molecular crowding significantly stabilizes G-quadruplexes of various G-rich sequences, but destabilizes duplexes,[40−42] which leads to a structural change between the duplex and quadruplexes of G-rich and complementary C-rich sequences.[43,44] It is important to note that the molecular crowding effects on G-quadruplex conformation largely depend on the loop length and sequence. Just a single nucleotide difference in a loop of a G-quadruplex results in drastic differences in its conformation and thermodynamics under molecular crowding conditions.[45,46] However, how the loops affect the conformation, thermodynamics, and hydration of G-quadruplexes is not yet completely understood.

In this article, to elucidate the critical roles of loops that determine the conformation and thermodynamics of G-quadruplexes under molecular crowding conditions, we designed DNA sequences with different numbers of G-quartets and thymines in each loop, and investigated their conformation and thermodynamics under dilute and molecular crowding conditions with PEG 200 (poly(ethylene glycol) with an average molecular weight of 200). As a result, we found that G-quadruplexes with shorter loops predominantly underwent structural transitions from antiparallel or mixed to parallel conformations upon molecular crowding in the presence of Na^+ or K^+. Thermodynamic parameters showed that there was an optimal loop size to maximize G-quadruplex stability in the presence of Na^+. Moreover, we found that the number of water molecules released from a G-quadruplex in the presence of Na^+ decreased with increasing thermodynamic stability under the dilute condition. These results suggest a thermodynamics-hydration relationship of the loops which dominates the conformation and thermodynamics of G-quadruplexes under molecular crowding conditions.

2. EXPERIMENTAL SECTION

2.1. Materials. Natural DNA oligonucleotides were HPLC grade and were purchased from Hokkaido System Science (Sapporo, Japan). DNA oligonucleotides containing abasic sites were synthesized by a normal solid-phase synthetic procedure. For the abasic sites (nucleotides without bases) dSpacer CE Phosphoramidite (GLEN, Sterling, Virginia) was used. After purification using a C18 column and polyacrylamide gel (acrylamide:bis(acrylamide) = 19:1) electrophoresis in 7 M urea, the single-strand concentrations of the DNA oligonucleotides were determined by measuring the absorbance at 260 nm at 90 °C using a Shimadzu 1700 spectrophotometer (Shimadzu, Kyoto, Japan) connected to a thermo programmer. Single-strand extinction coefficients were calculated from mononucleotide and dinucleotide data using the nearest-neighbor approximation.[47]

2.2. Circular Dichroism Measurements. Circular dichroism (CD) experiments utilizing a JASCO J-820 spectropolarimeter (JASCO, Hachioji, Japan) were measured in a 0.1 cm path length cuvette for 40 μM total strand concentration of DNA. All measurements were carried out in buffers of 100 mM NaCl, 10 mM Na_2HPO_4 (pH 7.0), and 1 mM Na_2EDTA or 100 mM KCl, 10 mM K_2HPO_4 (pH 7.0), and 1 mM K_2EDTA containing various concentrations of PEG 200 at 4 °C. The CD spectra were obtained by taking the average of at least three scans made from 200 to 350 nm. The temperature of the cell holder was regulated by a JASCO PTC-348 temperature controller, and the cuvette-holding chamber was flushed with a constant stream of dry N_2 gas to avoid condensation of water on the cuvette exterior. Before the measurement, the sample was heated to 90 °C, gently cooled at a rate of 0.5 °C min^{-1}, and incubated at 4 °C for several hours.

2.3. Gel Electrophoresis. Native gel electrophoresis was carried out on nondenaturing gels containing 10% polyacrylamide. Ice-cold loading buffer (3 μL) was mixed with 3 μL of 5 μM DNA sample in the buffer of 100 mM NaCl, 10 mM Na_2HPO_4 (pH 7.0), and 1 mM Na_2EDTA at 0 wt % and 40 wt % PEG 200. A 4 μL aliquot of the mixed solution was loaded and analyzed by electrophoresis (5 V cm^{-1} for 3h at 4 °C). Gels were stained using SYBR Gold (Life Technologies Corporation, California, U.S.A.) and imaged using FLA-7000 (GE Healthcare Co., Ltd., Tokyo, Japan). Before the measurement the sample was heated to 90 °C, gently cooled at a rate of 0.5 °C min^{-1}, and incubated at 4 °C for several hours.

2.4. Thermodynamic Analyses. The UV melting curves of DNA oligonucleotides were measured by a Shimadzu 1700 spectrophotometer (Shimadzu, Kyoto, Japan) equipped with a temperature controller. The UV melting curves of G-quadruplexes were measured at 295 nm where G-quadruplexes show a hypochromic transition.[48,49] All experiments were carried out in the buffers of 100 mM NaCl, 10 mM Na_2HPO_4 (pH 7.0), and 1 mM Na_2EDTA or 100 mM KCl, 10 mM K_2HPO_4 (pH 7.0), and 1 mM K_2EDTA containing various concentrations of PEG 200. The heating and cooling rates were 0.5 °C min^{-1}. The thermodynamic parameters were calculated

dx.doi.org/10.1021/jp308402v | J. Phys. Chem. B 2013, 117, 963−972

Table 1. Oligonucleotides Used in This Study

abbreviation	sequence
G2T2	5′-GGTTGGTTGGTTGG-3′
G2T3	5′-GGTTTGGTTTGGTTTGG-3′
G2T4	5′-GGTTTTGGTTTTGGTTTTGG-3′
G2T5	5′-GGTTTTTGGTTTTTGGTTTTTGG-3′
G2T6	5′-GGTTTTTTGGTTTTTTGGTTTTTTGG-3′
G3T2	5′-GGGTTGGGTTGGGTTGGG-3′
G3T3	5′-GGGTTTGGGTTTGGGTTTGGG-3′
G3T4	5′-GGGTTTTGGGTTTTGGGTTTTGGG-3′
G3T5	5′-GGGTTTTTGGGTTTTTGGGTTTTTGGG-3′
G3T6	5′-GGGTTTTTTGGGTTTTTTGGGTTTTTTGGG-3′
G4T2	5′-GGGGTTGGGGTTGGGGTTGGGG-3′
G4T3	5′-GGGGTTTGGGGTTTGGGGTTTGGGG-3′
G4T4	5′-GGGGTTTTGGGGTTTTGGGGTTTTGGGG-3′
G4T5	5′-GGGGTTTTTGGGGTTTTTGGGGTTTTTGGGG-3′
G4T6	5′-GGGGTTTTTTGGGGTTTTTTGGGGTTTTTTGGGG-3′
G2Φ2T2	5′-GGΦΦTTGGΦΦTTGGΦΦTTGG-3′
G2Φ4	5′-GGΦΦΦΦGGΦΦΦΦGGΦΦΦΦGG-3′

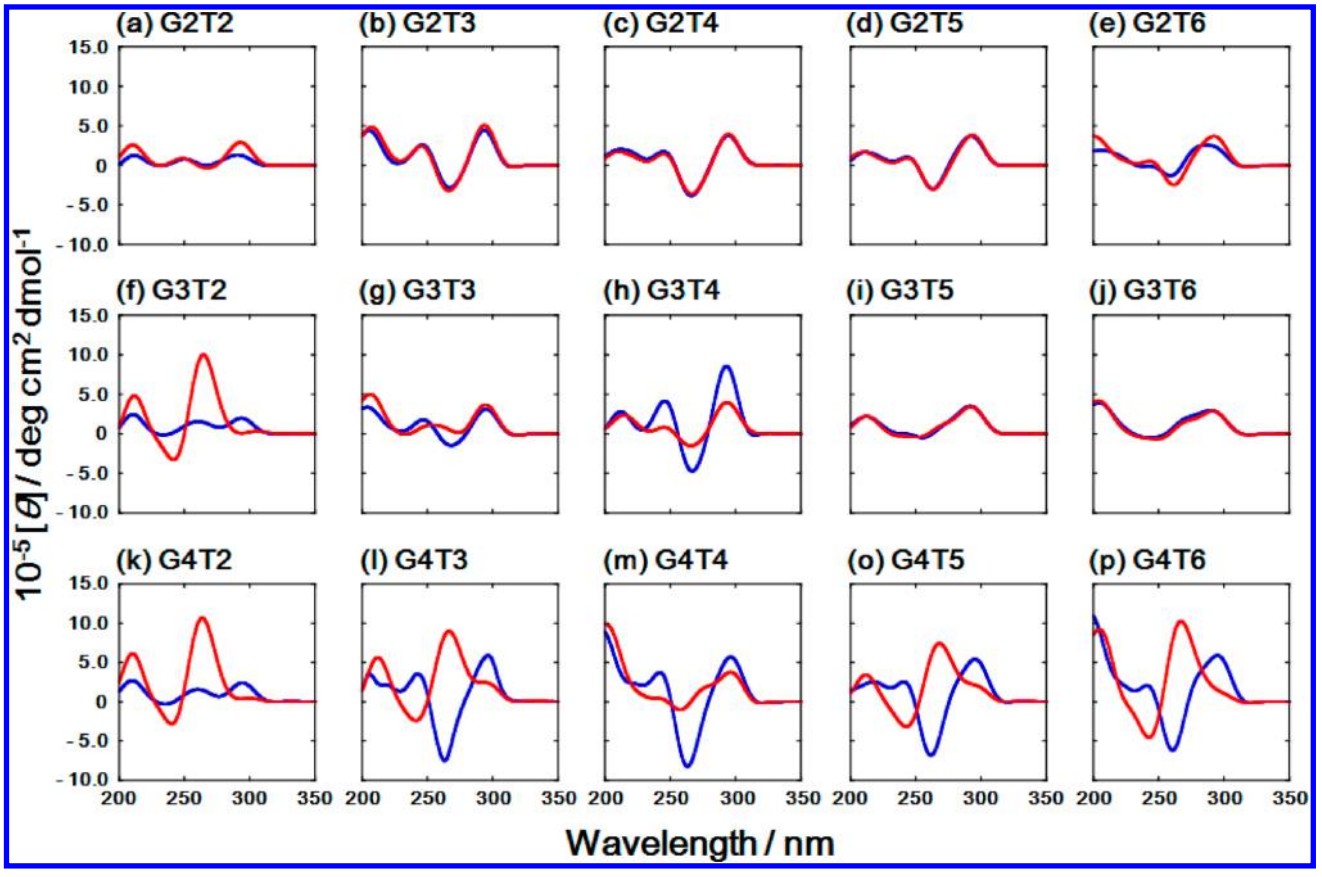

Figure 2. CD spectra of 40 μM G2T2 (a), G2T3 (b), G2T4 (c), G2T5 (d), G2T6 (e), G3T2 (f), G3T3 (g), G3T4 (h), G3T5 (i), G3T6 (j), G4T2 (k), G4T3 (l), G4T4 (m), G4T5 (n), and G4T6 (o) in the buffer of 100 mM NaCl, 10 mM Na_2HPO_4 (pH 7.0), and 1 mM Na_2EDTA at 0 wt % (blue) or 40 wt % PEG 200 (red). All measurements were carried out at 4 °C.

from the fit of the melting curves (with at least five different concentrations of DNA oligonucleotides) to a theoretical equation for an intramolecular association as described previously.[47] Note that the thermodynamic analysis in this study is based on the van't Hoff equation. The van't Hoff equation assumes that the transition equilibrium involves only two states (i. e., G-quadruplex and random coil), and the difference in the heat capacities (ΔC_p) of these states is zero.[50,51] If these assumptions are not established, the thermodynamic parameters are not accurate. Thus, it is necessary to show evidence for a two-state transition of the heat denaturation and renaturation of the DNA G-quadruplexes in the experimental conditions. Before the measurement, the sample was heated to 90 °C, gently cooled at a rate of 0.5 °C min^{-1}, and incubated at 0 °C for several hours.

2.5. Water Activity Measurements. The water activity was determined by the osmotic stress method via vapor phase osmometry using a model 5520XR pressure osmometer

dx.doi.org/10.1021/jp308402v | J. Phys. Chem. B 2013, 117, 963−972

(Wescor, Utah, U.S.A.) with the assumption that the cosolutes do not directly interact with DNAs.[40,52]

3. RESULTS

3.1. Sequence Design. The purpose of this study is to show the effects of loop length on the conformation, thermodynamic stability, and hydration of DNA G-quadruplexes. For this purpose, it is necessary to systematically design G-quadruplex-forming DNA sequences with different lengths of the guanine stretch and loop. In order to fold into an intramolecular G-quadruplex, at least four guanine stretches and three connecting loops are required. The length of the guanine stretch can be varied from two to four bases as shown in the thrombin binding aptamer and *Oxytricha nova* and other telomere sequences. On the other hand, variety in the length and sequence of the loops has been reported in naturally occurring G-quadruplex-forming DNA sequences. In order to eliminate sequence-specific effects of the loop, which may induce particular conformation and thermodynamic properties in the G-quadruplex, we introduced two to six thymines as the loop sequences. Consequently, the DNA oligonucleotides designed here have different numbers of G-quartets and thymines in each loop [G*m*T*n*: *m* indicates the number of G-quartets ($2 \leq m \leq 4$) and *n* indicates the number of thymines in each loop ($2 \leq n \leq 6$)]. The sequences and abbreviations are listed in Table 1.

3.2. G-Quadruplex Conformation Dependence on the Nucleotide Sequences and Solution Conditions. We initially studied the folding topologies of G*m*T*n* by CD spectroscopy. Figure 2 shows CD spectra of the DNA sequences in the buffer of 100 mM NaCl, 10 mM Na_2HPO_4 (pH 7.0), and 1 mM Na_2EDTA at 0 wt % PEG 200 (blue lines) and 40 wt % PEG 200 (red lines) as the dilute and molecular crowding conditions, respectively. The CD signature consisting of positive and negative peaks around 295 and 260 nm, respectively, indicates a typical antiparallel conformation.[53] On the other hand, a CD spectrum with positive and negative peaks at 260 and 240 nm, respectively, indicates a parallel conformation.[54] The presence of two positive peaks at 295 and 260 nm indicates a mixed [(3 + 1), hybrid] conformation.[55] Although CD intensity depends on the DNA sequence, we found that G2T2, G2T3, G2T4, G2T5, G2T6, and G3T4 folded into an antiparallel conformation under both dilute and molecular crowding conditions. G3T5 and G3T6 folded into a mixed conformation under both conditions. On the other hand, G3T2, G4T2, G4T3, G4T5, and G4T6 underwent a conformational transition from an antiparallel or a mixed to a parallel conformation by molecular crowding. G3T3 and G4T4 underwent a conformational transition from an antiparallel to a mixed one. The G-quadruplex conformations and the conformational transitions induced by molecular crowding depend on the combination of numbers of G-quartets and loop lengths. Under the dilute condition, most of the sequences folded into an antiparallel conformation, and some of them folded into a mixed conformation. Under the molecular crowding condition, the DNA sequences with larger numbers of G-quartets and smaller numbers of thymines folded into parallel or mixed conformations. In addition, we studied the conformations of G*m*T*n* in the presence of 100 mM KCl (Figure S1). For G2T*n*, CD spectra in the presence of K^+ were very similar with those in the presence of Na^+. We found that G3T*n*, except G3T2, underwent a conformational transition from a mixed or an antiparallel conformation to a parallel conformation by molecular crowding. G3T2 formed a parallel conformation in both conditions. In G4T*n*, G4T3, G4T4, and G4T5 underwent a conformational transition from a mixed to a parallel conformation by molecular crowding. G4T2 and G4T6 folded into a parallel conformation under both conditions. From these results, we concluded that the molecular crowding effects on the conformations in the presence of Na^+ and K^+ are similar to each other; molecular crowding induces the parallel conformation as previously demonstrated by NMR for human telomere DNA sequences.[36] In addition, we found that a parallel conformation is more favored in the presence of K^+ than in the presence of Na^+, although G2T*n* maintained the antiparallel conformation even under the molecular crowding condition. Thus, we concluded that DNA sequences with larger numbers of G-quartets and smaller numbers of thymines had induced conformational transitions by molecular crowding. These results are useful in predicting how molecular crowding affects G-quadruplex conformation.

3.3. Thermodynamics of G-Quadruplexes with Different Loop Length under Dilute and Molecular Crowding Conditions. Next, we studied the effects of loop length on the thermodynamics of G-quadruplexes utilizing G2T*n*, because their conformations were not altered by molecular crowding. The molecularity of G2T*n* was confirmed by native PAGE under both dilute and molecular crowding conditions (Figure 3), and a single band was observed for both. The migration of

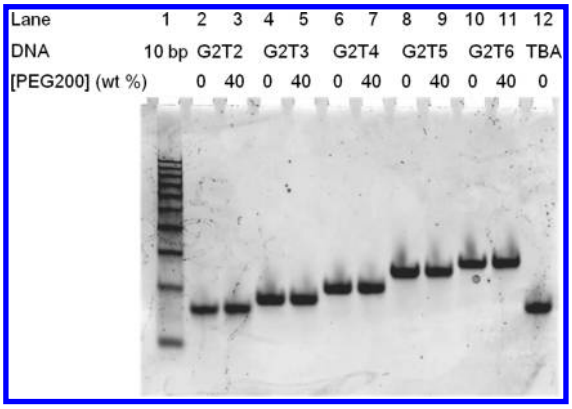

Figure 3. Native gel electrophoresis of the G-quadruplex on a 10% polyacrylamide gel in the following buffer: 100 mM NaCl, 10 mM Na_2HPO_4 (pH 7.0), and 1 mM Na_2EDTA with 0 wt % PEG 200 (lanes 2, 4, 6, 8, 10, and 12) or 40 wt % PEG 200 (lanes 3, 5, 7, 9, and 11) at 4 °C. Lane 1 contains a 10-bp DNA ladder. Lanes 2 and 3 contain G2T2. Lanes 4 and 5 contain G2T3. Lanes 6 and 7 contain G2T4. Lanes 8 and 9 contain G2T5. Lanes 10 and 11 contain G2T6. Lane 12 contains the thrombin binding aptamer (15-mer).

G2T2 was the same as the thrombin binding aptamer (15 mer), which folds into an intramolecular G-quadruplex. In addition, the migrations of G2T*n* (n = 2−6) continuously changed depending on the length. These results show that G2T*n* forms an intramolecular G-quadruplex as we designed, although it is possible that some of them are not stable enough under the conditions.

Figure 4 shows the normalized UV melting curves of G2T*n* under the dilute (blue lines) and molecular crowding (red lines) conditions in the presence of Na^+. We confirmed that there was no hysteresis for any sequence at 0 and 40 wt % PEG 200 (Figures S2 and S3), supporting the two-state transition of the G-quadruplexes under experimental conditions. The T_m

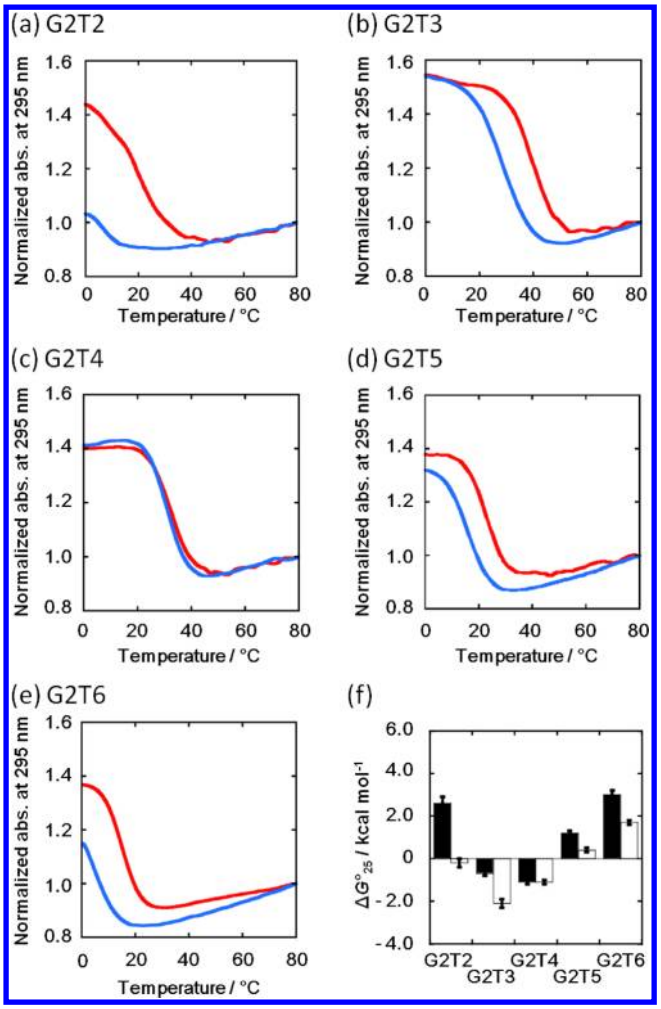

Figure 4. Normalized UV melting curves at 295 nm of 5 μM G2T2 (a), G2T3 (b), G2T4 (c), G2T5 (d), and G2T6 (e) in the buffer of 100 mM NaCl, 10 mM Na_2HPO_4 (pH 7.0), and 1 mM Na_2EDTA at 0 wt % PEG 200 (blue) and at 40 wt % PEG 200 (red). (f) Values of ΔG°_{25} for G-quadruplexes of G2T2, G2T3, G2T4, G2T5, and G2T6 in the buffer of 100 mM NaCl, 10 mM Na_2HPO_4 (pH 7.0), and 1 mM Na_2EDTA at 0 wt % PEG 200 (solid bar) and at 40 wt % PEG 200 (open bar).

values of G2T2, G2T3, G2T4, G2T5, and G2T6 were evaluated as 7.3, 28.6, 30.7, 16.7, and 8.2 °C, respectively, under the dilute condition (Table 2). In order to confirm the T_m values, we further evaluated T_m by the use of a dA/dT plot (data not shown). The T_m values evaluated by the curve fitting procedure and the dA/dT plot were consistent with each other (differences for G2T2 and G2T6 were 0.3 and 3.7 °C, respectively). The thermal stability of the G-quadruplexes increased with an increasing number of thymines in each loop from two to four. On the other hand, it decreased with an increasing number of thymines in each loop from four to six. The values rose to 24.9, 40.0, 32.7, 23.0, and 15.7 °C, respectively, under the molecular crowding condition. These results qualitatively showed that the G-quadruplexes were thermally stabilized by molecular crowding.

We further attempted to quantify the loop length effects on the thermodynamics. Table 2 shows the values of free energy change at 25 °C (ΔG°_{25}), the enthalpy change (ΔH°), and the entropy change at 25 °C ($T\Delta S^\circ$) for the formation of G-quadruplexes under the dilute and molecular crowding conditions in the presence of Na^+. When the length of each loop increased from two to four, the values of ΔG°_{25} under the dilute condition decreased from +2.6 ± 0.3 to −1.1 ± 0.1 kcal mol^{-1} (Figure 4f). In contrast, with an increased loop length from four to six, the values of ΔG°_{25} increased from −1.1 ± 0.1 to +3.0 ± 0.2 kcal mol^{-1}. The values of ΔG°_{25} varied from −1.1 to +3.0 kcal mol^{-1} depending on the loop length. These parameters showed that the loop length largely determines the thermodynamics of the whole G-quadruplex.

The loop length of the most stable G-quadruplex under the dilute condition is different from that under the molecular crowding condition. The effect of molecular crowding on the thermodynamics was evaluated as follows: $\Delta\Delta G^\circ_{25} = \{\Delta G^\circ_{25(40wt\%PEG200)}\} - \{\Delta G^\circ_{25(0wt\%PEG200)}\}$. In the presence of 100 mM Na^+, the value of $\Delta\Delta G^\circ_{25}$ for G2T2 was −2.8 kcal mol^{-1}. This negative value of $\Delta\Delta G^\circ_{25}$ quantitatively shows that molecular crowding stabilizes the G-quadruplex. By comparing $\Delta\Delta G^\circ_{25}$ for G2T*n* (G2T2, −2.8 kcal mol^{-1}; G2T3, −1.4 kcal mol^{-1}; G2T4, 0.0 kcal mol^{-1}; G2T5, −0.8 kcal mol^{-1}; and G2T6, −1.3 kcal mol^{-1}), the degree of the stabilization by molecular crowding decreased with an increase of loop length from two to four and increased with an increase of loop length from four to six. The values of ΔH° and $T\Delta S^\circ$ further indicate that the promotion of G-quadruplex formation by molecular crowding is due to the favorable enthalpic contribution that exceeds the unfavorable entropic contribution. The enthalpic stabilization of G-quadruplexes by molecular crowding agrees with previous reports showing a stabilization effect of molecular crowding for the thrombin binding aptamer forming antiparallel G-quadruplexes (33). Notably, the minimum values of

Table 2. Thermodynamic Parameters for the Formation of G-Quadruplexes in the Presence of 100 mM Na^+[a]

abbreviation	[PEG200]/wt %	T_m/°C	ΔG°_{25}/kcal mol^{-1}	ΔH°/kcal mol^{-1}	$T\Delta S^\circ$/kcal mol^{-1}
G2T2	0	7.3	+2.6 ± 0.3	−47.6 ± 6.0	−50.2 ± 6.5
	40	24.9	−0.2 ± 0.2	−39.8 ± 2.7	−39.6 ± 2.6
G2T3	0	28.6	−0.7 ± 0.1	−37.2 ± 1.0	−36.5 ± 1.1
	40	40.0	−2.1 ± 0.2	−45.5 ± 2.1	−43.3 ± 2.1
G2T4	0	30.7	−1.1 ± 0.1	−50.4 ± 1.2	−49.3 ± 1.2
	40	32.7	−1.1 ± 0.1	−48.7 ± 1.6	−47.6 ± 1.6
G2T5	0	16.7	+1.2 ± 0.1	−45.0 ± 1.8	−46.1 ± 1.8
	40	23.0	+0.4 ± 0.1	−52.4 ± 1.0	−52.7 ± 1.0
G2T6	0	8.2	+3.0 ± 0.2	−50.2 ± 2.1	−53.2 ± 2.2
	40	15.7	+1.7 ± 0.1	−54.5 ± 3.2	−56.2 ± 3.2

[a]All experiments were carried out in a buffer containing 100 mM NaCl, 10 mM Na_2HPO_4 (pH 7.0), and 1 mM Na_2EDTA at 0 or 40 wt % PEG 200. Thermodynamic parameters are the average values obtained from melting curves with at least five concentrations of DNA oligonucleotides.

dx.doi.org/10.1021/jp308402v | J. Phys. Chem. B 2013, 117, 963−972

$\Delta G^{\circ}_{25(0wt\%PEG200)}$ and the maximum for $\Delta\Delta G^{\circ}_{25}$ were observed in G2T4, suggesting that there is a relationship between the thermodynamics and the molecular crowding effects on the thermodynamics of G-quadruplexes of G2T*n*.

In addition, we further measured melting and annealing curves of G2T*n* in the presence of 100 mM KCl (Figures S4 and S5). Hysteresis between the melting and annealing curves was observed for G2T2, indicating a nontwo-state transition. Moreover, biphasic melting and annealing transitions were observed for G2T4, showing that the denaturation and renaturation of G2T4 are not two-state. On the other hand, G2T3, G2T5, and G2T6 did not show hysteresis and biphasic transition, suggesting the two-state transition of these DNA sequences. Thus, we evaluated thermodynamic parameters of G-quadruplexes of these DNA sequences. The values of ΔG°_{25} of G2T3, G2T5, and G2T6 under the dilute condition were -3.5 ± 0.2, -0.2 ± 0.1, and $+1.1 \pm 0.1$ kcal mol^{-1}, respectively (Table S1). Under the molecular crowding condition, these values were -5.0 ± 0.2, -0.9 ± 0.1, and $+0.3 \pm 0.2$ kcal mol^{-1}, respectively. Comparing these parameters in the presence of Na^+ and K^+, the G-quadruplex structures of G2T3, G2T5, and G2T6 in the presence of K^+ were more stable than those in the presence of Na^+, although systematic comparison for the other sequences were not possible.

3.4. Hydration of G-Quadruplexes Depending on Loop Length. Since it is generally considered that the hydration change upon DNA folding is a major determinant of the molecular crowding effects on DNA structures,[36,46,52,56] we further investigated the hydration states of the G-quadruplexes of G2T*n*. UV melting analyses as a function of PEG 200 concentration were performed. The relationship between thermodynamics ($\ln K_{obs}$) and the water activity ($\ln a_w$) in the presence of 100 mM Na^+ is shown in Figure 5a. The plots

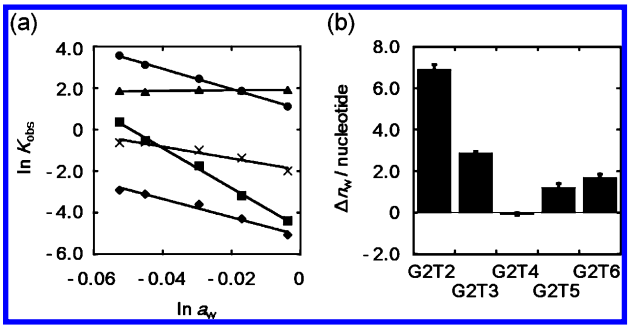

Figure 5. (a) Plots of $\ln K_{obs}$ versus $\ln a_w$ for G2T2 (■), G2T3 (●), G2T4 (▲), G2T5 (×), or G2T6 (♦) in the buffer of 100 mM NaCl, 10 mM Na_2HPO_4 (pH 7.0), and 1 mM Na_2EDTA at 0, 10, 20, 30, and 40 wt % PEG 200 at 25 °C. (b) Values of Δn_w for G2T2, G2T3, G2T4, G2T5, and G2T6.

reveal that the thermodynamics of G-quadruplexes ($\ln K_{obs}$) decrease linearly with the increase in $\ln a_w$. These linear relationships suggest that the slope is approximately equal to the number of water molecules released upon the G-quadruplex folding, $-\Delta n_w$.[40] The slopes of the plot in Figure 5a for G2T2, G2T3, G2T5, and G2T6 provided a negative value of $-\Delta n_w$, meaning a release of water molecules during G-quadruplex formation.[40,52] In the case of G2T4, the thermodynamic stability of the G-quadruplex was almost independent of the water activity, suggesting almost no water uptake or release upon formation. The values of Δn_w per nucleotide of G2T2, G2T3, G2T4, G2T5, and G2T6 for the formation of G-quadruplexes were $+6.9 \pm 0.2$, $+2.9 \pm 0.1$, -0.1 ± 0.1, $+1.2 \pm 0.2$, and $+1.7 \pm 0.2$, respectively, in the presence of 100 mM Na^+ (Figure 5b). The value of Δn_w decreased with an increasing loop length from two to four, and increased with an increasing loop length from four to six. Comparing Δn_w (Figure 5b) and ΔG°_{25} (Figure 4f) under the dilute condition, the lower thermodynamic stability leads to the larger number of water molecules released (e.g., G2T2 and G2T6). In contrast, the stable G-quadruplex structures under the dilute condition release fewer water molecules upon folding (e.g., G2T4). These results raise the question of how the loop length regulates the thermodynamics and hydration of G-quadruplexes. Moreover, the values of Δn_w of G2T3, G2T5, and G2T6 in the presence of 100 mM K^+ were evaluated to be $+2.7 \pm 0.3$, $+1.1 \pm 0.3$, and $+1.2 \pm 0.2$. The values of Δn_w in the presence of K^+ were similar with those in the presence of Na^+. These results are consistent with the hydration change for the G-quadruplex of the thrombin binding aptamer in the presence of K^+ and Na^+.[52] Although the thermodynamics-hydration relationship in the presence of K^+ could not be confirmed because of the nontwo-state transition of G2T2 and G2T4, it is reasonable to conclude that the observations are independent of the coexisting cation.

3.5. Thermodynamics-Hydration Relationship of G-Quadruplex Loops. Figure 6 shows the loop structures of two, three, and four thymine loops in $(T_2G_4)_4$, $(G_4T_3G_4)_2$, and $(G_4T_4)_3G_4$, respectively.[57−59] Since a loop with two thymine bases (T2 loop) is too short to form stacking interactions between thymine bases in the loop and guanine bases in the neighboring G-quartet, the T2 loop is in a disordered structure

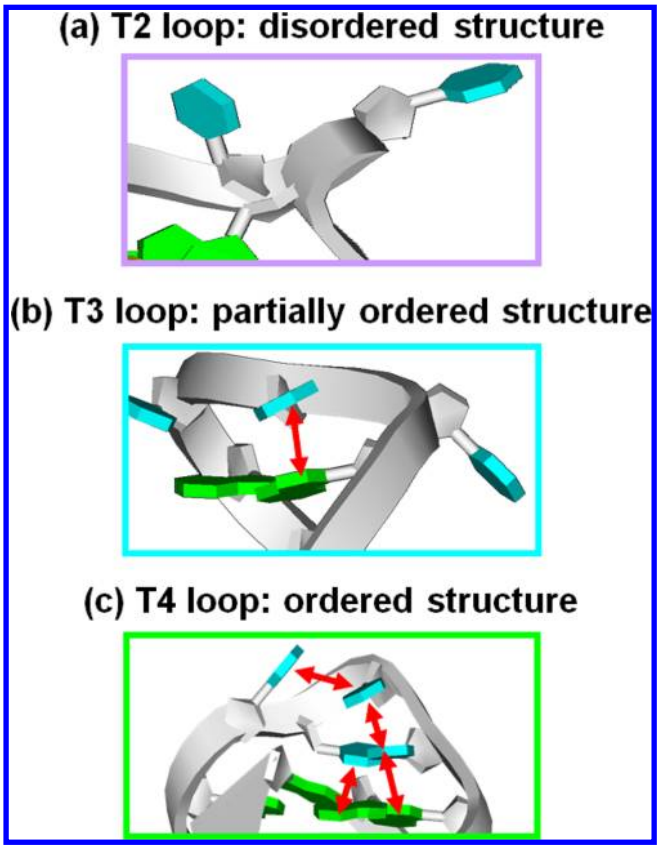

Figure 6. Three-dimensional structure of the T2 loop (PDB ID: 186D) (a), T3 loop (PDB ID: 2avh) (b), and T4 loop (PDB ID: 201D) (c).

dx.doi.org/10.1021/jp308402v | J. Phys. Chem. B 2013, 117, 963−972

(Figure 6a). Such disordered loops result in an unstable G-quadruplex structure. The degree of the order in the loop further affects the hydration. Since the disordered structure is relatively flexible, the functional groups, which can be hydrogen bonding donors and acceptors, are not in a certain orientation, and there should be fewer binding sites in the disordered loop. Note that there are water molecules taken up and released through the folding of DNA structures; water molecules should be taken up in the grooves to form a spine of water.[60−63] On the other hand, water molecules bound to functional groups in bases used for base pair formation should be released through the structure formation. The disordered loops can reduce the water molecules taken up, and as a result, accelerate the dehydration of the whole G-quadruplex structure.

In contrast, a loop with four thymine bases (T4 loop) forms a stacking interaction network among thymine bases in the loop and guanine bases in the neighboring G-quartet as shown in Figure 6c.[57] The well-ordered bases in the T4 loops contribute to stabilization of the G-quadruplex structure. Moreover, such an ordered loop structure accumulates functional groups that can be binding sites for water molecules. The bound water molecules may become a scaffold for a secondary hydration shell as shown in the case of the duplex.[60] Thus, the ordered loops increase the number of water molecules taken up upon folding and reduce the dehydration of the whole G-quadruplex structure. A loop with three thymine bases (T3 loop) is in between the T2 and T4 loops. The T3 loop is in a partially ordered structure, in which one of the three bases forms a stacking interaction with the neighboring G-quartet, resulting in a moderate effect on the thermodynamics and hydration of the G-quadruplex. These results demonstrate for the first time a relationship between the thermodynamics and hydration of the loops in G-quadruplexes, linked via stacking interactions formed among thymine bases in the loop and guanine bases in the neighboring G-quartet.

3.6. Effects of Stacking Interactions on the Thermodynamics and Hydration of G-Quadruplexes. In order to validate the thermodynamics−hydration relationship, we further designed and synthesized DNA oligonucleotides with abasic nucleotides (Φ shown in Figure 7a), G2Φ2T2 (5′-GGΦΦTTGGΦΦTTGGΦΦTTGG-3′ loops are underlined) and G2Φ4 (5′-GGΦΦΦΦGGΦΦΦΦGGΦΦΦΦGG-3′ loops are underlined), because abasic nucleotides cannot form stacking interactions. Comparing G2T4, G2Φ4, and G2Φ2T2, the loops of G2Φ4 cannot form any stacking interactions in the loops, whereas G2Φ2T2 may partly form stacking interactions (Figure 7b−d).

The conformations of G2Φ2T2 and G2Φ4 were studied by CD spectroscopy at 0 and 40 wt % PEG 200 (Figure 8a,b) in the buffer of 100 mM NaCl, 10 mM Na_2HPO_4 (pH 7.0), and 1 mM Na_2EDTA. The CD spectra of G2Φ2T2 under the dilute condition (blue line) and the molecular crowding condition (red line) are similar with the CD spectra of G2T4 under the same conditions, indicating an antiparallel conformation of G2Φ2T2. The CD spectrum of G2Φ4 under the dilute condition did not show the signature for the antiparallel conformation, whereas the typical CD spectrum for the antiparallel conformation was observed under the molecular crowding condition. This should be due to an unstable structure of G2Φ4 under dilute conditions (see below). These results showed that the conformations of G2Φ2T2 and G2Φ4 are similar with that of G2T4, indicating that abasic nucleotides in the loop do not affect the whole G-quadruplex structure.

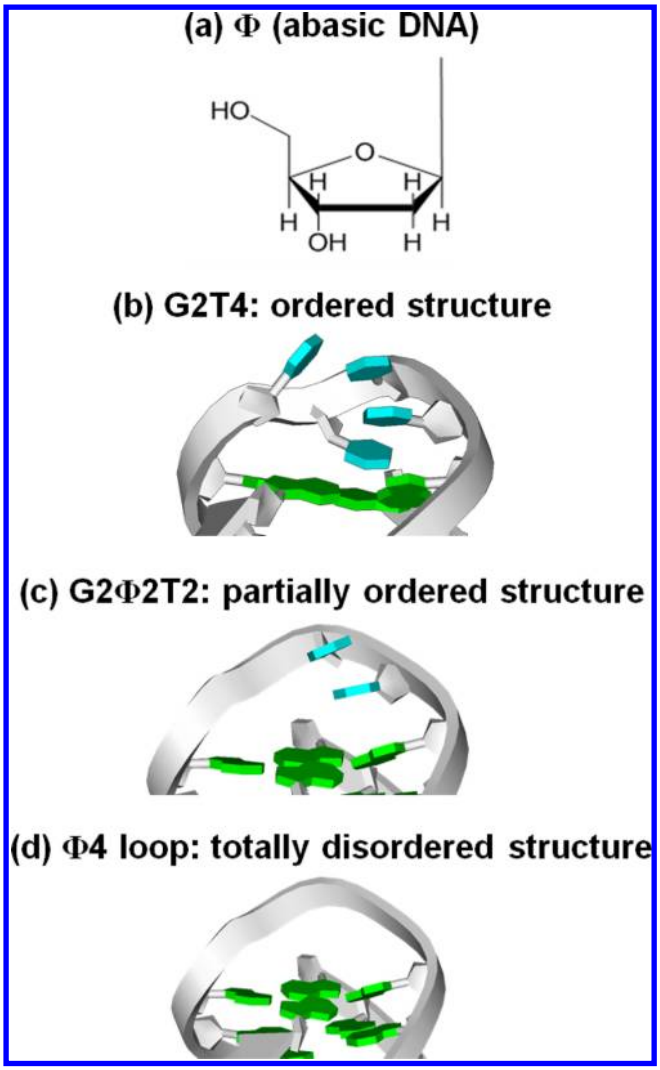

Figure 7. Chemical structure of abasic DNA (a), schematic structure of loops of G2T4 (b), G2Φ2T2 (c), and G2Φ4 (d).

Figure 8c shows UV melting curves of G2Φ2T2 in the buffer of 100 mM NaCl, 10 mM Na_2HPO_4 (pH 7.0), and 1 mM Na_2EDTA at 0 wt % PEG 200 (blue) and 40 wt % PEG 200 (red) under the dilute and molecular crowding conditions, respectively. The T_m under the dilute condition was 31.8 °C, according to the dA/dT plot shown in the inset of Figure 8c. This T_m is slightly higher that of G2T3 (Figure 4b). The T_m of G2Φ2T2 under the molecular crowding condition was 30.2 °C. Thus, molecular crowding slightly destabilizes the G-quadruplex of G2Φ2T2, indicating that just a few water molecules are taken up upon G-quadruplex folding. In the case of G2Φ4, the hypochromic transition at 295 nm that is typical for G-quadruplex unfolding was not observed under the dilute condition (Figure 8d). This indicates that G2Φ4 cannot form a stable G-quadruplex, even at low temperatures, and that the T_m is considerably lower than 0 °C. This is consistent with the structural analysis by CD spectroscopy (Figure 8b). In contrast, a clear hypochromic transition was observed under the molecular crowding condition, and the T_m was around 4.7 °C (inset of Figure 8d). From these melting curves, we found that molecular crowding with PEG 200 significantly stabilized the

dx.doi.org/10.1021/jp308402v | J. Phys. Chem. B 2013, 117, 963−972

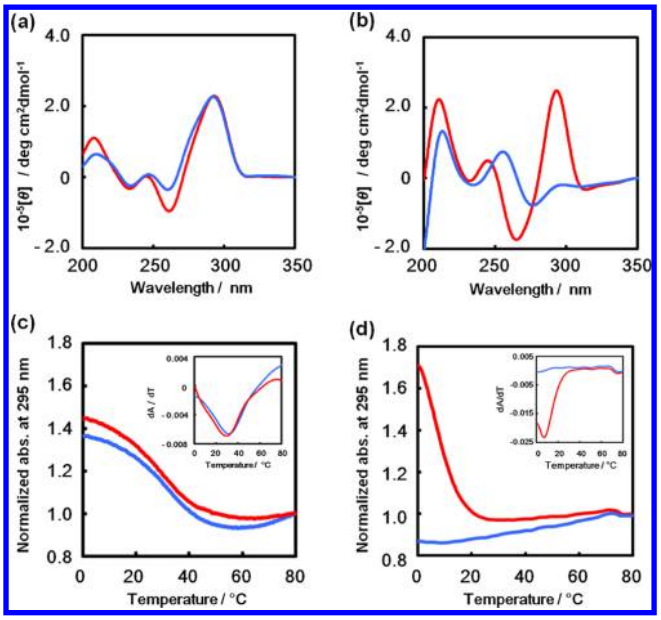

Figure 8. CD spectra for 40 μM G2Φ2T2 (a) and G2Φ4 (b) in the buffer of 100 mM NaCl, 10 mM Na_2HPO_4 (pH 7.0), and 1 mM Na_2EDTA at 0 wt % (blue) or 40 wt % PEG 200 (red). Normalized UV melting curves for 40 μM of G2Φ2T2 (c) and G2Φ4 (d) in the buffer of 100 mM NaCl, 10 mM Na_2HPO_4 (pH 7.0), and 1 mM Na_2EDTA at 0 wt % (blue) or 40 wt % PEG 200 (red). Inset: dA/dT plots for G2Φ2T2 (c) and G2Φ4 (d) in the buffer of 100 mM NaCl, 10 mM Na_2HPO_4 (pH 7.0), and 1 mM Na_2EDTA at 0 wt % (blue) or 40 wt % PEG 200 (red).

antiparallel G-quadruplex of G2Φ4. The difference between the T_m values of G2Φ4 under the dilute and molecular crowding conditions was at least 10 °C, which was the most significant stabilization effect by molecular crowding compared with G2T*n*. A larger stabilization (a larger difference in ln K_{obs}) by molecular crowding indicates more water molecules released upon folding. Although ln K_{obs} of the antiparallel G-quadruplex of G2Φ4 cannot be estimated because of the low stability, these results strongly indicated that the most unstable G-quadruplex of G2Φ4 under the dilute condition released the largest number of water molecules through folding. By comparing the thermal stability of G2T4, G2Φ2T2, and G2Φ4, the order of the thermodynamic stability was as follows: G2T4 ≈ G2Φ2T2 ≫ G2Φ4. Moreover, the number of water molecules released upon folding was in the order G2Φ4 ≫ G2Φ2T2 ≈ G2T4. Thus, we conclude that a more unstable G-quadruplex with disordered loops, due to fewer stacking interactions, is more significantly stabilized by molecular crowding, corresponding to more water molecules being released upon folding. This supports the hypothesized relationship between the thermodynamics and hydration of the loops in G-quadruplexes as described above.

4. DISCUSSION

Thermodynamic analyses of G-quadruplexes of G2T*n* (n = 2–6) revealed that the structure of the loop, the nonbase-paired region, in the G-quadruplex is critical in determining not only the thermodynamic stability but also the hydration of the whole G-quadruplex. The enthalpy changes of the G2T*n* G-quadruplexes under the dilute condition show that the loop stabilizes the G-quadruplex by favorable enthalpy contributions (Table 2), although the enthalpy changes of G2T2 and G2T6 do not follow this rule. This could be due to uncertainty of the curve fitting procedure since the T_ms are too low and the lower base lines are not enough to evaluate precise parameters for the enthalpy and entropy changes, even though the free energy change, which correlates the T_m value, is usually relatively accurate. The favorable enthalpic contribution of the loops suggests that the thymine bases within the loops and the guanine bases of the neighboring G-quartet form stacking interactions. The ordered structure of the loop regions can be scaffolds for the binding of water molecules, resulting in more hydration upon G-quadruplex folding. The molecular crowding effects on the thermal stability of G-quadruplexes of DNA sequences with abasic sites in the loops further support the thermodynamic-hydration relationship within the loop. Such a relationship between the loop structure and hydration number was previously reported for G-quadruplexes of the thrombin binding aptamer and with modified loop sequences.[33] It has been shown that hydration differences, depending on loop substitutions, are associated with the stacking interactions within the loops.[33] Thus, the thermodynamic-hydration relationship of the loop is applicable for different base contexts including adenine, cytosine, thymine, and other non-natural bases. In addition, the effects of molecular crowding on the conformation and stability of G-quadruplexes with abasic sites at different positions have been examined.[64] In that study, a systematic comparison of the effects of molecular crowding and abasic sites on the thermodynamic parameters showed that the effects of molecular crowding on the thermodynamics of G-quadruplex formation were determined by the enthalpy change during formation, which depended on the position of the abasic site.[64] The degree of the molecular crowding effect on the thermodynamics reflected the degree of the hydration. Thus, abasic sites in G-quartet also showed the thermodynamics–hydration relationship as observed for the loop. These results indicate that the structure of nonbase-paired regions in a G-quadruplex critically affects the thermodynamics and hydration of the whole G-quadruplex.

Importantly, the relationship has been observed for DNA duplexes with various nonbase-paired regions such as hairpin loops, mismatches, and non-natural nucleotide analogues within the duplex motif.[63] In that study, the authors found that there was no water binding to less-ordered sites, such as flexible loops and unpaired mismatch pairs, whereas stable loops and paired mismatches took up larger numbers of water molecules upon duplex formation. Given these results for DNA G-quadruplexes and duplexes, it is possible to posit that the nonbase-paired regions in the DNA structure critically affect not only the thermodynamics but also the hydration of the whole structure. Since thermodynamically stable structures serve as a scaffolding for water molecules, more stable non-base-paired structures attract more water molecules upon structure formation, leading to more hydration. More hydration results in larger destabilization of the whole DNA structure under molecular crowding conditions, where the water activity and concentration are reduced by osmolytes.

5. CONCLUSIONS

We systematically designed G-quadruplexes with various numbers of G-quartet planes and thymine bases in each loop, G*m*T*n*, and studied the molecular crowding effects on their conformation and thermodynamic stability. The conformations and conformational transitions induced by molecular crowding depended on a combination of the number of G-quartets and

dx.doi.org/10.1021/jp308402v | J. Phys. Chem. B 2013, 117, 963–972

loop length. DNA sequences with a larger number of G-quartets and a smaller number of thymines had induced conformational transitions by molecular crowding. Moreover, thermodynamic analyses showed a relationship between the thermodynamics and hydration of the loops in the G-quadruplex, linked via stacking interactions formed among thymine bases in the loop and guanine bases in the neighboring G-quartet. Since thermodynamically stable structures serve as a scaffolding for water molecules, a more stable nonbase-paired structure attracts more water molecules upon structure formation, leading to more hydration. Although other types of nonbase-paired regions in various DNA structures should be studied, these results give important insights into the native structure of DNA under molecular crowding conditions, which is an important cellular environmental factor. Moreover, the molecular crowding effects on the thermodynamics of DNA structures are applicable in the design and development of biological assays, biosensors, and molecular devices under intracellular conditions.

■ ASSOCIATED CONTENT

Supporting Information

Thermodynamic parameters for the formation of G-quadruplexes in the presence of 100 mM K^+ (Table S1). CD spectra the compounds (Figure S1). Normalized UV melting (blue) and annealing (red) curves (Figures S2−S5). This material is available free of charge via the Internet at http://pubs.acs.org.

■ AUTHOR INFORMATION

Corresponding Author

*Tel: +81-078-303-1426. Fax: +81-078-303-1495. E-mail: miyoshi@center.konan-u.ac.jp.

Notes

The authors declare no competing financial interest.

■ ACKNOWLEDGMENTS

This work was supported in part by Grants-in-Aid for Scientific Research, the Scientific Research on Innovative Areas "Nanomedicine Molecular Science" (No. 2306), and the "Strategic Research Foundation at Private Universities" (2009-2014) from the Ministry of Education, Culture, Sports, Science and Technology, Japan, and the Hirao Taro Foundation of the Konan University Association for Academic Research. T.F. received a Research Fellowship from the Japan Society for the Promotion of Science for Young Scientists.

■ REFERENCES

(1) Sen, D.; Gilbert, W. *Nature* **1988**, *334*, 364−366.
(2) Williamson, J. R. *Annu. Rev. Biophys. Biomol. Struct.* **1994**, *23*, 703−730.
(3) Gellert, M.; Lipsett, M. N.; Davies, D. R. *Proc. Natl. Acad. Sci. U.S.A.* **1962**, *48*, 2013−2018.
(4) Simonsson, T. *Biol. Chem.* **2001**, *382*, 621−628.
(5) Keniry, M. A. *Biopolymers* **2001**, *56*, 123−146.
(6) Sen, D.; Gilbert, W. *Methods Enzymol.* **1992**, *211*, 191−199.
(7) Kankia, B. I.; Marky, L. A. *J. Am. Chem. Soc.* **2001**, *123*, 10799−10804.
(8) Blackburn, E. H. *Nature* **1991**, *350*, 569−573.
(9) Patel, D. J.; Phan, A. T.; Kuryavyi, V. *Nucleic Acids Res.* **2007**, *35*, 7429−7455.
(10) Huppert, J. L. *Biochimie* **2008**, *90*, 1140−1148.
(11) Fedoroff, O. Y.; Salazar, M.; Han, H.; Chemeris, V. V.; Kerwin, S. M.; Hurley, L. H. *Biochemistry* **1998**, *37*, 12367−12374.
(12) Han, F. X.; Wheelhouse, R. T.; Hurley, L. H. *J. Am. Chem. Soc.* **1999**, *121*, 3561−3570.
(13) Wei, C.; Jia, G.; Yuan, J.; Feng, Z.; Li, C. *Biochemistry* **2006**, *45*, 6681−6691.
(14) Gonçalves, D. P.; Ladame, S.; Balasubramanian, S.; Sanders, J. K. *Org. Biomol. Chem.* **2006**, *4*, 3337−3342.
(15) Yaku, H.; Murashima, T.; Miyoshi, D.; Sugimoto, N. *Chem. Commun.* **2010**, *46*, 5740−5742.
(16) Ueyama, H.; Takagi, M.; Takenaka, S. *J. Am. Chem. Soc.* **2002**, *124*, 14286−14287.
(17) Xiao, Y.; Piorek, B. D.; Plaxco, K. W.; Heeger, A. J. *J. Am. Chem. Soc.* **2005**, *127*, 17990−17991.
(18) Miyoshi, D.; Inoue, M.; Sugimoto, N. *Angew. Chem., Int. Ed.* **2006**, *45*, 7716−7719.
(19) Miyoshi, D.; Karimata, H.; Wang, Z. M.; Koumoto, K.; Sugimoto, N. *J. Am. Chem. Soc.* **2007**, *129*, 5919−5925.
(20) Chen, C.; Zhao, C.; Yang, X.; Ren, J.; Qu, X. *Adv. Mater.* **2010**, *22*, 389−393.
(21) Chang, H.; Tang, L.; Wang, Y.; Jiang, J.; Li, J. *Anal. Chem.* **2010**, *82*, 2341−2346.
(22) Ge, B.; Huang, Y. C.; Sen, D.; Yu, H. Z. *Angew. Chem., Int. Ed.* **2010**, *49*, 9965−6697.
(23) Dutta, K.; Fujimoto, T.; Inoue, M.; Miyoshi, D.; Sugimoto, N. *Chem. Commun.* **2010**, *46*, 7772−7774.
(24) Wu, L.; Wang, J.; Feng, L.; Ren, J.; Wei, W.; Qu, X. *Adv. Mater.* **2012**, *24*, 2447−2452.
(25) Macaya, R. F.; Schultze, P.; Smith, F. W.; Roe, J. A.; Feigon, J. *Proc. Natl. Acad. Sci. U.S.A.* **1993**, *90*, 3745−3749.
(26) Wang, Y.; Patel, D. J. *Structure* **1993**, *1*, 263−282.
(27) Parkinson, G. N.; Lee, M. P.; Neidle, S. *Nature* **2002**, *417*, 876−880.
(28) Risitano, A.; Fox, K. R. *Biochemistry* **2003**, *42*, 6507−6513.
(29) Risitano, A.; Fox, K. R. *Nucleic Acids Res.* **2004**, *32*, 2598−2606.
(30) Hazel, P.; Huppert, J.; Balasubramanian, S.; Neidle, S. *J. Am. Chem. Soc.* **2004**, *126*, 16405−16415.
(31) Bugaut, A.; Balasubramanian, S. *Biochemistry* **2008**, *47*, 689−697.
(32) Guédin, A.; Alberti, P.; Mergny, J. L. *Nucleic Acid Res.* **2009**, *37*, 5559−5567.
(33) Olsen, C. M.; Lee, H. T.; Marky, L. A. *J. Phys. Chem. B* **2009**, *113*, 2587−2595.
(34) Li, J.; Correia, J. J.; Wang, L.; Trent, J. O.; Chaires, J. B. *Nucleic Acids Res.* **2005**, *33*, 4649−4659.
(35) Phan, A. T. *FEBS J.* **2010**, *277*, 1107−1117.
(36) Heddi, B.; Phan, A. T. *J. Am. Chem. Soc.* **2011**, *133*, 9824−9833.
(37) Ellis, R. J.; Minton, A. P. *Nature* **2003**, *425*, 27−28.
(38) Al-Habori, M. *Int. J. Biochem. Cell Biol.* **2001**, *33*, 844−864.
(39) Miyoshi, D.; Sugimoto, N. *Biochimie* **2008**, *90*, 1040−1051.
(40) Nakano, S.; Karimata, H.; Ohmichi, T.; Kawakami, J.; Sugimoto, N. *J. Am. Chem. Soc.* **2004**, *126*, 14330−14331.
(41) Xue, Y.; Kan, Z. Y.; Wang, Q.; Yao, Y.; Liu, J.; Hao, Y. H.; Tan, Z. *J. Am. Chem. Soc.* **2007**, *129*, 11185−11191.
(42) Miller, M. C.; Buscaglia, R.; Chaires, J. B.; Lane, A. N.; Trent, J. O. *J. Am. Chem. Soc.* **2010**, *132*, 17105−17107.
(43) Miyoshi, D.; Matsumura, S.; Nakano, S.; Sugimoto, N. *J. Am. Chem. Soc.* **2004**, *126*, 165−169.
(44) Kan, Z. Y.; Yao, Y.; Wang, P.; Li, X. H.; Hao, Y. H.; Tan, Z. *Angew. Chem., Int. Ed.* **2006**, *45*, 1629−1632.
(45) Miyoshi, D.; Karimata, H.; Sugimoto, N. *Angew. Chem., Int. Ed.* **2005**, *44*, 3740−3744.
(46) Arora, A.; Maiti, S. *J. Phys. Chem. B* **2009**, *113*, 8784−8792.
(47) Sugimoto, N.; Nakano, S.; Katoh, M.; Matsumura, A.; Nakamuta, H.; Ohmichi, T.; Yoneyama, M.; Sasaki, M. *Biochemistry* **1995**, *34*, 11211−11216.
(48) Mergny, J. L.; Phan, A. T.; Lacroix, L. *FEBS Lett.* **1998**, *435*, 74−78.
(49) Mergny, J. L.; Li, J.; Lacroix, L.; Amrane, S.; Chaires, J. B. *Nucleic Acids Res.* **2005**, *33*, e138−e143.
(50) Petersheim, M.; Turner, D. H. *Biochemistry* **1983**, *22*, 256−263.

(51) Freier, S. M.; Sugimoto, N.; Sinclair, A.; Alkema, D.; Neilson, T.; Kierzek, R.; Caruthers, M. H.; Turner, D. H. *Biochemistry* **1986**, *25*, 3214−3219.
(52) Miyoshi, D.; Karimata, H.; Sugimoto, N. *J. Am. Chem. Soc.* **2006**, *128*, 7957−7963.
(53) Chen, F. M. *Biochemistry* **1992**, *31*, 3769−3776.
(54) Lu, M.; Guo, Q.; Kallenbach, N. R. *Biochemistry* **1993**, *32*, 598−601.
(55) Xu, Y.; Noguchi, Y.; Sugiyama, H. *Bioorg. Med. Chem.* **2006**, *14*, 5584−5591.
(56) Miller, M. C; Buscaglia, R.; Chaires, J. B.; Lane, A. N.; Trent, J. O. *J. Am. Chem. Soc.* **2010**, *132*, 17105−17107.
(57) Wang, Y.; Patel, D. J. *Structure* **1994**, *2*, 1141−1156.
(58) Wang, Y.; Patel, D. J. *J. Mol. Biol.* **1995**, *251*, 76−94.
(59) Hazel, P.; Parkinson, G. N.; Neidle, S. *J. Am. Chem. Soc.* **2006**, *128*, 5480−5487.
(60) Denisov, V. P.; Carlström, G.; Venu, K.; Halle, B. *J. Mol. Biol.* **1997**, *268*, 118−136.
(61) Feig, M.; Pettitt, B. M. *J. Mol. Biol.* **1999**, *286*, 1075−1095.
(62) Privalov, P. L.; Dragan, A. I.; Crane-Robinson, C.; Breslauer, K. J.; Remeta, D. P.; Minetti, C. A. *J. Mol. Biol.* **2007**, *365*, 1−9.
(63) Nakano, S.; Hirayama, H.; Miyoshi, D.; Sugimoto, N. *J. Phys. Chem. B* **2012**, *116*, 7406−7415.
(64) Fujimoto, T.; Nakano, S.; Miyoshi, D.; Sugimoto, N. *J. Nucleic Acids* **2011**, 857149.